

Nucleon deformation and atomic spectroscopy ¹

A.J. Buchmann

Institute for Theoretical Physics, University of Tübingen

Auf der Morgenstelle 14, D-72076 Tübingen, Germany

e-mail:alfons.buchmann@uni-tuebingen.de

Abstract

Recent inelastic electron-proton scattering experiments have led to rather accurate values for the $N \rightarrow \Delta$ transition quadrupole moment $Q_{N \rightarrow \Delta}$. The experimental results imply a prolate (cigar-shaped) intrinsic deformation of the nucleon. The nonsphericity of the proton's charge distribution might be seen in the spectrum of atomic hydrogen. The possibilities and limitations for determining the geometric shape of the nucleon in an atomic physics experiment are discussed.

1 Introduction

Elastic electron-proton scattering experiments and atomic spectroscopy measurements have shown that the positive charge of the proton is distributed over a finite volume, and that the charge radius of the proton is about $r_p = 0.9$ fm [1]. Furthermore, the proton's radial charge density $\rho(r)$ could be determined from the Fourier transform of the charge form factor measured in elastic electron-proton scattering. However, the proton charge distribution most certainly has an angular dependence, i.e., $\rho(\mathbf{r}) = \rho(r, \Theta)$. This angular dependence of the proton charge density is not directly accessible in elastic scattering.

Inelastic photon and electron scattering experiments provide further details about the inner structure of the nucleon. In particular they show that the proton has a spectrum of excited states. When photons of sufficient energy impinge on a hydrogen target, the proton may be excited to its lowest lying excited state with spin 3/2, called the $\Delta^+(1232)$, where the number in parentheses is the energy (mass) of this state in units of MeV. The Δ^+ resonance decays quickly via the strong interaction into the proton ground state of 939 MeV and the lightest strongly interacting particle, the pion, with a mass of about 140 MeV. The lifetime of the Δ^+

¹published in Can. J. Phys. **83**, 455 (2005).

is of the order of 10^{-23} s, i.e., the time it takes for a gluon to travel across the proton radius of 10^{-15} m. This corresponds to a line width of about 100 MeV.

From a multipole analysis of the electromagnetic $p \rightarrow \Delta^+$ transition amplitude we have inferred that the proton charge density deviates from spherical symmetry. In fact, recent experimental determinations of the $p \rightarrow \Delta^+$ transition quadrupole moment [2, 3, 4] provide evidence for a prolate (cigar-shaped) intrinsic deformation of the proton [5].

2 Structure of the nucleon

2.1 Quark model

The structure of the nucleon² ground state and its excitation spectrum is explained in the quark model [6]. In the quark model the proton and neutron consist of three spin 1/2 quarks which come in two charge states, called up and down quarks, i.e., $p(uud)$ and $n(ddu)$. Here, u and d denote the up-quark with electric charge $e_u = 2/3$ and down-quark with charge $e_d = -1/3$. The first excited states of the proton and neutron, the $\Delta^+(uud)$ and $\Delta^0(ddu)$ with spin $J = 3/2$, have the same quark content as the p and n with spin $J = 1/2$. Thus we expect the properties of the Δ to be closely related to those of the N ground state. Formally, N and Δ properties are related because there exists a higher symmetry than isospin, called SU(6) spin-flavor symmetry, which combines the N isospin doublet with $J = 1/2$, and the Δ isospin quartet with $J = 3/2$ together with other states in the same 56-dimensional spin-flavor supermultiplet.

The strong interaction between the quarks is modelled as a long range harmonic oscillator confinement force, which guarantees that the colored quarks cannot be observed as free particles. In order to explain the spectrum in greater detail, for example, the mass splitting between the $N(939)$ with spin 1/2 and the $\Delta(1232)$ with spin 3/2 (see Fig. 1), the long-range spin-independent confinement forces must be supplemented by short-range spin-dependent terms. Spin-dependent forces arise, e.g., from one-gluon exchange between quarks. The one-gluon

²The proton and neutron, which have nearly the same mass of about 939 MeV can (with respect to strong interactions) be regarded as one particle, called nucleon $N(939)$, that exists in two charge states. Similarly, the first excited state of the nucleon, the $\Delta(1232)$ exists in four charge states $\Delta^-, \Delta^0, \Delta^+, \Delta^{++}$, which are energetically almost degenerate, i.e., all four states have a mass of about 1232 MeV. Mathematically, this symmetry is described by the SU(2) isospin group, whose generators are, in analogy to the spin, the Pauli matrices. The N has isospin 1/2 and the Δ has isospin 3/2. The quarks building up the N and Δ have approximately the same mass and thus have isospin 1/2.

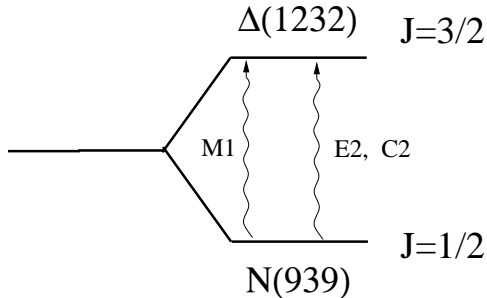


Figure 1: The hyperfine splitting between the $N(939)$ and $\Delta(1232)$ due to the spin-dependent interaction between quarks. This splitting is the nucleon physics analogue of the 21 cm line between the hyperfine states $F = 0$ and $F = 1$ in atomic hydrogen. In nucleon spectroscopy, an excited state is usually denoted by the name of the resonance followed by its energy [MeV] in parentheses.

exchange potential (OGEP) is analogous to the Fermi-Breit interaction between the electron and proton in atomic hydrogen, except for a factor $\boldsymbol{\lambda}_i \cdot \boldsymbol{\lambda}_j$, which reflects that quarks carry color charges, and the replacement of the photon-electron coupling constant α by the strong gluon-quark coupling α_s . The most important terms of the one-gluon exchange potential (spin-orbit terms are omitted) are

$$V^{OGEP}(\mathbf{r}_i, \mathbf{r}_j) = \frac{\alpha_s}{4} \boldsymbol{\lambda}_i \cdot \boldsymbol{\lambda}_j \left\{ \frac{1}{r} - \frac{\pi}{m_q^2} \left(1 + \frac{2}{3} \boldsymbol{\sigma}_i \cdot \boldsymbol{\sigma}_j \right) \delta(\mathbf{r}) - \frac{1}{4m_q^2} \frac{1}{r^3} (3\boldsymbol{\sigma}_i \cdot \hat{\mathbf{r}} \boldsymbol{\sigma}_j \cdot \hat{\mathbf{r}} - \boldsymbol{\sigma}_i \cdot \boldsymbol{\sigma}_j) \right\}. \quad (1)$$

Here, $\mathbf{r} = \mathbf{r}_i - \mathbf{r}_j$ is the distance between the i -th and j -th quark; $\hat{\mathbf{r}} = \mathbf{r}/r$ is the corresponding unit vector, $\boldsymbol{\sigma}_i$ is the spin operator (Pauli matrices), and $\boldsymbol{\lambda}_i$ is the color operator (Gell-Mann matrices). The constituent quark mass of the up and down quarks is denoted as m_q . Usually one chooses $m_q = M_N/3$ where M_N is the nucleon mass. In the entire paper we use natural units $\hbar = c = 1$.

The $1/r$ term is called color-Coulomb interaction, and the $\boldsymbol{\sigma}_i \cdot \boldsymbol{\sigma}_j$ term is referred to as color-magnetic interaction. The matrix element of the operator $\boldsymbol{\lambda}_i \cdot \boldsymbol{\lambda}_j$ between color singlet states, such as the N and Δ , is readily evaluated and gives a factor $-8/3$. Therefore, the color magnetic interaction is repulsive between quark pairs coupled to spin 1 and attractive between quark pairs coupled to spin 0.

The mass difference between the N and Δ masses of 293 MeV is almost completely determined by the color-magnetic interaction in Eq.(1); the $N - \Delta$ mass difference is often referred to as hyperfine splitting (see Fig. 1) in analogy to the 10^{-6} eV splitting between the $F = 0$ and

$F = 1$ hyperfine states in the hydrogen atom ground state. The huge difference of fourteen orders of magnitude between the hyperfine splitting in the nucleon and hydrogen atom is mainly due to the different size of both systems³.

2.2 The electromagnetic $N \rightarrow \Delta$ transition

If the Δ resonance is produced in an electromagnetic process (see Fig. 2), parity invariance and angular momentum conservation restrict the $N \rightarrow \Delta$ excitation to magnetic dipole (M1), electric quadrupole (E2), and charge or (Coulomb) quadrupole (C2) transitions. Although the E2 and C2 amplitudes are small (about 1/40 of the dominant magnetic dipole transition amplitude) they are nevertheless important because their nonzeroness provides evidence for a deviation of the nucleon charge distribution from spherical symmetry [2, 3, 4, 5]. In the quark model, the $\Delta(1232)$ is obtained from the $N(939)$ ground state either by flipping the spin of a single quark (M1 transition) or by flipping the spins of two quarks (E2 or C2 transition) [7]. In the case of the quadrupole transitions there is also a small contribution coming from e.g., lifting a single quark from an S state in the nucleon into an orbitally excited D state in the Δ .

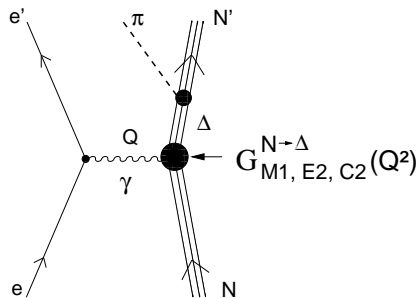


Figure 2: The excitation of the $\Delta(1232)$ resonance by a virtual photon γ of momentum Q is described by the three electromagnetic transition form factors $G_{M1}^{N \rightarrow \Delta}(Q^2)$, $G_{E2}^{N \rightarrow \Delta}(Q^2)$, and $G_{C2}^{N \rightarrow \Delta}(Q^2)$. Their contribution to the inelastic electron-nucleon cross section can be obtained by analyzing the angular distribution of the decay pions in coincidence with the scattered electron. In the limit $Q \rightarrow 0$, the cross section is described by the magnetic dipole moment $\mu_{N \rightarrow \Delta}$ and the charge quadrupole moment $Q_{N \rightarrow \Delta}$.

With the quark model it is also possible to calculate how much the proton charge distribution deviates from spherical symmetry and which degrees of freedom are responsible for

³The matrix element of the δ -function in Eq.(1) is proportional to $1/R^3$, where R is a measure of the spatial extension of the system, i.e., the quark core radius $b \approx 0.5$ fm in the case of the nucleon, and the Bohr radius $a_0 \approx 0.5 \text{ \AA}$ in the case of the hydrogen atom.

this deformation [5]. A multipole expansion of the nucleon charge density operator ρ up to quadrupole terms leads to the following invariants in spin-isospin space

$$\rho = A \sum_i^3 e_i - B \sum_{i<j}^3 e_i \left[2 \boldsymbol{\sigma}_i \cdot \boldsymbol{\sigma}_j - (3 \sigma_{iz} \sigma_{jz} - \boldsymbol{\sigma}_i \cdot \boldsymbol{\sigma}_j) \right], \quad (2)$$

where σ_{iz} is the z -component of the Pauli spin matrix of quark i , and $e_i = \frac{1}{6}(1 + \tau_{iz})$ is the quark charge where τ_{iz} is the third component of the Pauli isospin matrix. The constants A and B in front of the one- and two-quark terms parametrize the orbital and color matrix elements so that ρ is only an operator in spin-isospin space. It is important to note that the one-body operator (the A term) in Eq.(2) represents the valence quark degrees of freedom, whereas the two-body operator (the B term) even though it also acts on quark variables provides an effective description of the quark-antiquark degrees of freedom in the physical N and Δ [5, 8, 7]. Three-quark currents are omitted here, but were taken into account in Ref. [9].

After evaluating Eq.(2) between quark model spin-isospin wave functions the following relations between the p , n , and Δ^+ charge radii, and between the $p \rightarrow \Delta^+$ transition quadrupole moment $Q_{p \rightarrow \Delta^+}$ and the neutron charge radius r_n^2 were derived [7]

$$r_p^2 - r_{\Delta^+}^2 = r_n^2, \quad Q_{p \rightarrow \Delta^+} = \frac{1}{\sqrt{2}} r_n^2, \quad (3)$$

where r_p^2 and $r_{\Delta^+}^2$ are the proton and Δ^+ charge radii. Inserting the experimental neutron charge radius [10] $r_n^2 = -0.113(3) \text{ fm}^2$ in the second relation of Eq.(3) we obtain $Q_{p \rightarrow \Delta^+} = -0.08 \text{ fm}^2$. This agrees well with recent determinations of $Q_{p \rightarrow \Delta^+}$ from inelastic electron-proton scattering data which yield $Q_{p \rightarrow \Delta^+}(\text{exp}) = -0.0846(33) \text{ fm}^2$ [3], and $Q_{p \rightarrow \Delta^+}(\text{exp}) = -0.108(9) \text{ fm}^2$ [4]. The second relation is the zero momentum transfer limit of a more general relation between the $N \rightarrow \Delta$ charge quadrupole transition form factor $G_{C2}^{N \rightarrow \Delta}(Q^2)$ and the elastic neutron charge form factor $G_C^n(Q^2)$

$$G_{C2}^{N \rightarrow \Delta}(Q^2) = -\frac{3\sqrt{2}}{Q^2} G_C^n(Q^2), \quad (4)$$

which is experimentally satisfied for a wide range of momentum transfers [11].

These relations are a consequence of the underlying SU(6) spin-flavor symmetry and its breaking by the spin-dependent two-body terms in Eq.(2). As we have noted before, the spin-spin interaction in Eq.(1) is repulsive between quark pairs in a spin 1 state and attractive in

quark pairs with spin 0. This explains why the Δ^+ , which contains only quark pairs coupled to spin 1 is heavier than the proton. Similarly, the electromagnetic counterparts of these spin-dependent terms in Eq.(2) explain why $r_{\Delta^+}^2 > r_p^2$, why the neutron charge radius is negative, and why the neutron has a prolate intrinsic deformation. This can be qualitatively understood as follows. The two down quarks in the neutron are always in a spin 1 state⁴. Consequently, the spin-spin force pushes them further apart than an up-down quark pair. This results in an elongated (prolate) charge distribution with the up quark in the middle, and at the same time in a negative neutron charge radius. On the other hand, in the neutral Δ , where all quark pairs are in a spin 1 state, there is an equal distance between up-down and down-down quark pairs. This corresponds to an equilateral triangle (oblate) configuration of the charges and a zero charge radius of the neutral Δ (see Fig. 3).

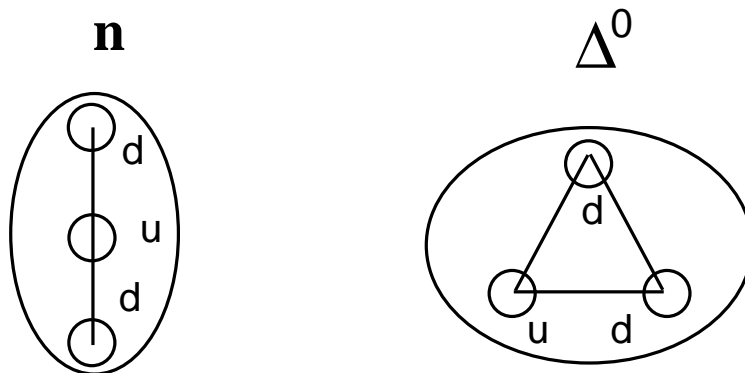


Figure 3: Qualitative picture of the neutron (left) and Δ^0 (right) charge distributions in the quark model. Although the deformation is depicted here as residing in the valence quark distribution, in reality a spherical quark core is surrounded by a deformed cloud of quarks and antiquarks [5]. A similar picture is obtained for the p and Δ^+ by interchanging u and d quarks.

⁴In order to satisfy the Pauli principle the total three-quark wave function, which is the direct product of orbital, spin-isospin, and color wave functions, must be completely antisymmetric under permutation of any two quarks. Because the color singlet N and Δ wave functions are antisymmetric in color space, the product of orbital and spin-isospin wave functions must be symmetric. For orbitally symmetric ground state S-wave functions this in turn means that the spin-isospin wave functions must be completely symmetric. The latter can only be achieved if the two down quarks in the neutron, which are necessarily in an isospin 1 state, are simultaneously in a spin 1 state.

3 Shape of the nucleon

3.1 Intrinsic quadrupole moment of the nucleon

In order to learn something about the shape of a spatially extended particle one has to determine its *intrinsic* quadrupole moment. The *intrinsic* quadrupole moment of a nucleus

$$Q_0 = \int d^3r \rho(\mathbf{r}) (3z^2 - r^2), \quad (5)$$

is defined with respect to the body-fixed frame. If the charge density is concentrated along the z -direction (symmetry axis of the particle), the term proportional to $3z^2$ dominates, Q_0 is positive, and the particle is prolate (cigar-shaped). If the charge density is concentrated in the equatorial plane perpendicular to z , the term proportional to r^2 prevails, Q_0 is negative, and the particle is oblate (pancake-shaped).

The intrinsic quadrupole moment Q_0 must be distinguished from the *spectroscopic* quadrupole moment Q measured in the laboratory frame. In the collective nuclear model [12], the relation between the observable spectroscopic quadrupole moment Q and the intrinsic quadrupole moment Q_0 is

$$Q = \frac{3K^2 - I(I+1)}{(I+1)(2I+3)} Q_0, \quad (6)$$

where I is the total spin of the nucleus, and K is the projection of I onto the z' -axis in the body fixed frame (symmetry axis of the nucleus)⁵. The factor between Q and Q_0 is due to the quantum mechanical precession of the deformed charge distribution with body-fixed symmetry axis z' around the lab frame z -axis along \mathbf{I}_z . Therefore, in the lab frame one does not measure the intrinsic quadrupole moment directly but only its projection onto the lab frame quantization axis. As can be seen from Eq.(6) a spin $I = 0$ nucleus does not have a spectroscopic quadrupole moment Q even if its intrinsic quadrupole moment Q_0 is different from zero. This is also the case for the spin $I = 1/2$ proton.

Recently, we have determined the intrinsic quadrupole moment of the proton and Δ^+ in the quark model [5] and found

$$Q_0^p = -r_n^2, \quad Q_0^{\Delta^+} = r_n^2, \quad (7)$$

⁵In the following the nuclear spin is denoted as \mathbf{I} and the total angular momentum of the electrons is denoted by \mathbf{J} .

i.e., the intrinsic quadrupole moment of the proton is given by the negative of the neutron charge radius and therefore positive, whereas the intrinsic quadrupole moment of the Δ^+ is negative. This corresponds to a prolate proton and an oblate Δ^+ deformation, consistent with the qualitative explanation given above.

The same result, namely a connection between the neutron charge radius r_n^2 and the intrinsic quadrupole moment of the proton Q_0^p is also obtained in the pion cloud model (see Fig. 4). In the pion cloud model, the nucleon consists of a spherically symmetric bare nucleon (quark core) surrounded by a pion with orbital angular momentum $l = 1$. For example, the neutron can be viewed as being composed of a bare proton surrounded by a negative pion. The nonspherical pion wave function leads to prolate intrinsic deformation of the nucleon. For further details see Ref. [5].

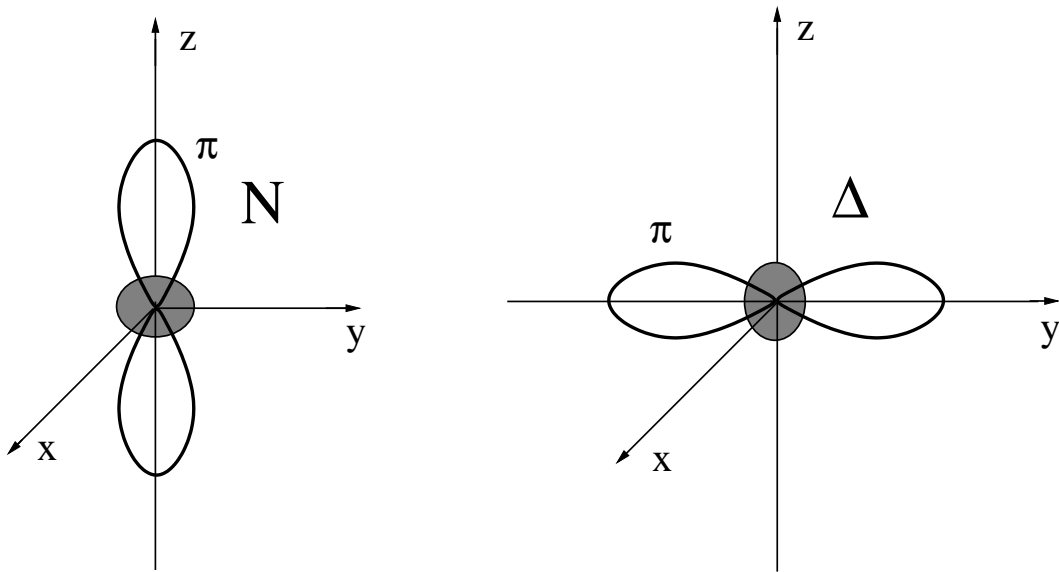


Figure 4: Intrinsic quadrupole deformation of the nucleon (left) and Δ (right) in the pion cloud model. In the N the p -wave pion cloud is concentrated along the polar (symmetry) axis, with maximum probability of finding the pion at the poles. This leads to a prolate deformation. In the Δ , the pion cloud is concentrated in the equatorial plane producing an oblate intrinsic deformation (from Ref. [5]).

Using for the nucleon the simple model of a homogeneously charged rotational ellipsoid, we can give Q_0 a geometric interpretation in terms of the half-axes of the ellipsoid. In classical electrodynamics the quadrupole moment of a rotational ellipsoid with charge Z , major axis a

along, and minor axis b perpendicular to the symmetry axis is given by

$$Q_0 = \frac{2Z}{5}(a^2 - b^2) = \frac{4}{5} Z R^2 \delta, \quad (8)$$

with the deformation parameter $\delta = 2(a - b)/(a + b)$ and the mean radius $R = (a + b)/2$. Inserting the quark model result $Q_0^p = -r_n^2 = 0.113 \text{ fm}^2$ on the left-hand side of Eq.(8), and for R the equivalent radius $R = \sqrt{5/3} r_p$, where r_p is the proton charge radius, we obtain a nucleon deformation parameter $\delta_N = 0.11$. This corresponds to a ratio of major to minor semi-axes $a/b = 1.11$. For the deformation parameter of the Δ we find $\delta_\Delta = -0.09$ and a half-axis ratio $a/b = 0.91$.

3.2 Intrinsic quadrupole charge density of the nucleon

To proceed, we decompose the proton charge form factor in two terms, a term resulting from a spherically symmetric charge distribution, and a second term due to the intrinsic quadrupole deformation of the actual charge density

$$G_C^p(Q^2) = G_{vol}^p(Q^2) - \frac{1}{6} Q^2 G_{def}^p(Q^2). \quad (9)$$

For the spherically symmetric part we take the usual dipole form factor $G_D(Q^2)$. Concerning the intrinsic quadrupole charge density, we employ the relation between the $N \rightarrow \Delta$ charge quadrupole transition form factor and the elastic neutron charge form factor in Eq.(4), and the relation between the intrinsic quadrupole moment of the nucleon and the neutron charge radius Eq.(7). We then obtain the following expressions

$$\begin{aligned} G_{vol}^p(Q^2) &= G_D(Q^2) = (1 + Q^2/\Lambda^2)^{-2}, & G_{def}^p(Q^2) &= -\sqrt{2} G_{C2}^{N \rightarrow \Delta}(Q^2) = \frac{6}{Q^2} G_C^n(Q^2) \\ G_C^p(Q^2) &= G_{vol}^p(Q^2) - G_C^n(Q^2), \end{aligned} \quad (10)$$

with $G_{def}^p(0) = Q_0^p$. Thus, the deviation of the neutron charge form factor from zero and the deviation of the nucleon's charge distribution from spherical symmetry are closely related.

According to Eq.(9) the proton charge density in coordinate space is decomposed in two parts, a spherically symmetric volume term $\rho_{vol}^p(r)$, and a nonspherical charge density denoted as $\rho_{def}^p(r)$

$$\rho^p(r) = \rho_{vol}^p(r) + \frac{1}{6} \nabla^2 \rho_{def}^p(r) = \rho_{vol}^p(r) - \rho^n(r), \quad (11)$$

where the last equality follows from Eq.(10). These coordinate space expressions show that the deviation of the proton charge density from spherical symmetry is described by the neutron charge density $\rho^n(r)$. To see the effect of the nucleon's nonsphericity explicitly, we use a two parameter fit [13] for the elastic neutron charge form factor

$$G_C^n(Q^2) = -\mu_n \frac{a\tau}{1+d\tau} G_D(Q^2), \quad (12)$$

where $\tau = Q^2/(4M_N^2)$ and $\Lambda^2 = 0.71 \text{ GeV}^2$. We then obtain for the Fourier transform of Eq.(12)

$$\rho^n(r) = \frac{1}{6} r_n^2 \frac{\Lambda^4 m^2}{4\pi(\Lambda^2 - m^2)^2} \left(m^2 \frac{e^{-mr}}{r} - \Lambda^2 \frac{e^{-\Lambda r}}{r} - (m^2 - \Lambda^2) \left(\frac{e^{-\Lambda r}}{r} - \frac{\Lambda}{2} e^{-\Lambda r} \right) \right), \quad (13)$$

where $m =: 2M_N/\sqrt{d}$. The neutron structure parameters a and d have been determined from the lowest moments of the experimental neutron charge form factor. They are given by the neutron charge radius r_n^2 , and the fourth moment r_n^4 [14]. Similarly, the Fourier transform of the intrinsic charge quadrupole form factor $G_{def}^p(Q^2)$ yields

$$\rho_{def}^p(r) = -r_n^2 \frac{\Lambda^4 m^2}{4\pi(\Lambda^2 - m^2)^2} \left(\frac{e^{-mr}}{r} - \frac{e^{-\Lambda r}}{r} - \frac{m^2 - \Lambda^2}{2\Lambda} e^{-\Lambda r} \right), \quad (14)$$

with $\int d^3r \rho_{def}^p(r) = Q_0^p = -r_n^2$. Finally, the spherically symmetric part of the proton charge density is obtained from the Fourier transform of the dipole form factor

$$\rho_{vol}^p(r) = \frac{\Lambda^3}{8\pi} e^{-\Lambda r}. \quad (15)$$

The decomposition of the proton charge density in a spherical volume part and a quadrupole deformation part is shown in Fig.5.

4 Atomic spectroscopy and nucleon structure

Before discussing the possibility of measuring the intrinsic quadrupole moment of the nucleon in an atomic physics experiment, I would like to recall that atomic spectroscopy provided the first clear evidence for nuclear quadrupole moments before these were seen with nuclear spectroscopic methods and nuclear scattering experiments. The quadrupole moment of the hydrogen isotope D was discovered using the molecular beam magnetic resonance method [15].

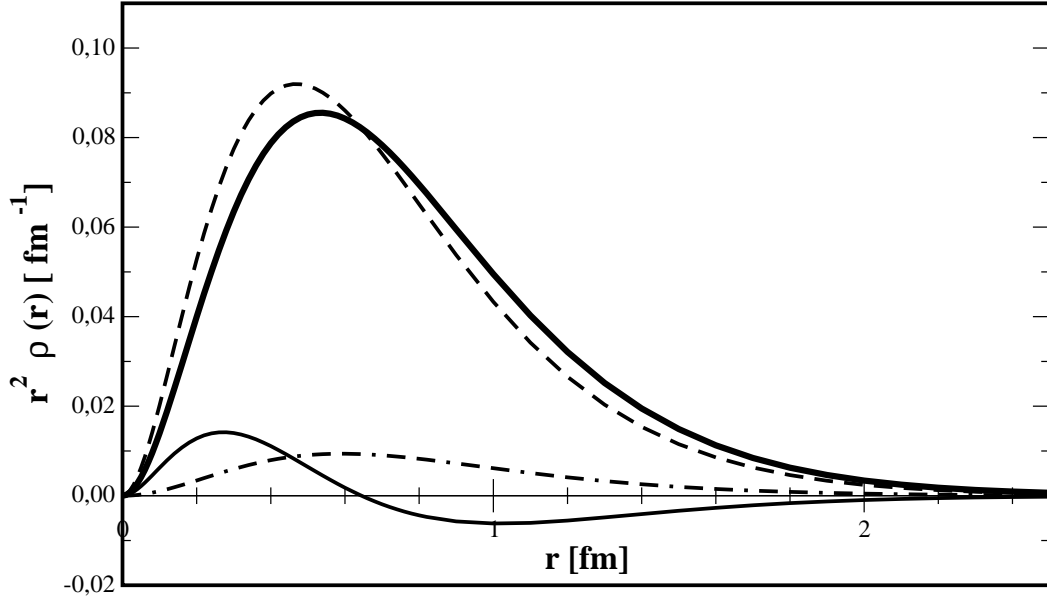


Figure 5: Spherically symmetric charge density of the proton $\rho_{vol}^p(r)$ [fm^{-3}] (broken curve); intrinsic quadrupole charge density of the nucleon $\rho_{def}^p(r)$ [fm^{-1}] (broken-dotted curve); neutron charge density $\rho^n(r) = -\frac{1}{6}\nabla^2\rho_{def}^p(r)$ (thin full curve); and the sum $\rho^p(r) = \rho_{vol}^p - \rho^n(r)$ (thick full curve). As a result of the intrinsic quadrupole deformation of the nucleon positive charge is moved to the exterior region of the proton. This will lead to a larger proton charge radius and will be discussed in sect. 4.3.

4.1 Discovery of nuclear quadrupole moments in atomic hyperfine spectra

Early in 1935, when measuring the magnetic hyperfine structure of certain atomic spectral lines of europium isotopes ^{151}Eu and ^{153}Eu with nuclear spin $I = 5/2$ Schüler and Schmidt found small but systematic deviations from the Landé interval rule [16]. The latter describes the magnetic hyperfine splitting of spectral lines due to the magnetic interaction energy between a nucleus with magnetic moment μ_I and spin \mathbf{I} , and the magnetic moment of the atomic electrons of total angular momentum \mathbf{J}

$$\Delta W_{hfs} = A \langle \mathbf{I} \cdot \mathbf{J} \rangle = \frac{1}{2} A C, \quad A = \mu_I H(0)/(IJ). \quad (16)$$

Here, A is a constant proportional to the magnetic field $H(0)$ produced by the atomic electrons at the site of the nucleus. Furthermore, $C = F(F + 1) - I(I + 1) - J(J + 1)$ is the Casimir factor where $\mathbf{F} = \mathbf{I} + \mathbf{J}$ is the sum of the nuclear and electronic angular momenta.

Schüler and Schmidt noted that their experimental results could be explained if a deviation of the nuclear charge distribution from spherical symmetry is assumed. The correct quantum

mechanical interpretation was given by Casimir [17] who showed that the observed hyperfine splitting pattern could be reproduced by adding a second term on the right hand side of Eq.(16) of the form

$$\Delta W_{hfs} = \frac{1}{2} AC + \frac{1}{8} B \frac{3C(C+1) - 4I(I+1)J(J+1)}{I(2I-1)J(2J-1)}, \quad B = Q \frac{\partial^2 \Phi}{\partial z^2}, \quad (17)$$

where the quadrupole constant B is given by the product of the nuclear quadrupole moment Q and the electric field gradient $\frac{\partial^2 \Phi}{\partial z^2}$ due to the electrons at the site of the nucleus. The quadrupole moment in Eq.(17) is referred to as the spectroscopic quadrupole moment. From the measured hyperfine splitting ΔW_{hfs} and the calculated electric field gradient the quadrupole moment Q could be determined. For the europium isotopes the result was $Q(^{151}\text{Eu}) = 150 \text{ fm}^2$ and $Q(^{153}\text{Eu}) = 320 \text{ fm}^2$.

For $I = 0$ and $I = 1/2$, Eq.(6) predicts $Q = 0$ and a vanishing quadrupole contribution to the hyperfine splitting ΔW_{hfs} even if the intrinsic quadrupole moment $Q_0 \neq 0$. Because of these selection rules it seems at first sight hopeless to obtain information on the shape of an $I = 1/2$ nucleus, such as the nucleon, from an atomic physics experiment. However, there are other observables that are sensitive to the geometric shape of the nucleus.

4.2 Isotope shifts and intrinsic quadrupole moments

The frequency of a certain spectral line of a given element is slightly different for the various isotopes of this element. These isotope shifts arise even in the absence of nuclear electromagnetic moments because different isotopes have different mass and size. Heavier isotopes with bigger radii experience less Coulomb binding than lighter isotopes with smaller radii, because the attractive inner atomic Coulomb potential is cut off near the surface of nucleus. Consequently the spectral lines of the heavier isotope are slightly shifted to lower frequencies compared to the same lines of the lighter isotope. For s electrons, the isotope shift is given by the following expression

$$\begin{aligned} \delta E_{IS} &= \frac{2\pi}{3} |\Psi_e(0)|^2 \delta \langle r^2 \rangle + \delta E_{mass} + \delta E_{pol}, \\ \delta \langle r^2 \rangle &= \delta \langle r^2 \rangle_{vol} + \delta \langle r^2 \rangle_{def} \end{aligned} \quad (18)$$

where $\delta \langle r^2 \rangle$ is the change in the nuclear charge radius of the two isotopes considered. Here, $\delta \langle r^2 \rangle_{vol}$ and $\delta \langle r^2 \rangle_{def}$ denote the volume and deformation contribution to the total

charge radius change. The electronic wave function at $r = 0$ is denoted as $\Psi_e(0) = \frac{1}{\pi}[Z/(na_0)]^3$, and a_0 is the Bohr radius. The terms δE_{mass} and δE_{pol} are the mass and nuclear polarization contributions to the isotope shift. In the following we discuss only the size (volume) and shape (deformation) contributions to the isotope shift.

If the radius change in Eq.(18) were a pure volume effect, we would expect the radius variation to be based on $R = R_0 A^{1/3}$, where A is the number of nucleons and $R_0 = 1.2$ fm. This relation between nuclear mass and equivalent radius $R = \sqrt{\frac{5}{3} \langle r^2 \rangle}$ follows from the nuclear liquid droplet model, which considers a nucleus as a spherical droplet of constant density. On the other hand, the deformation contribution to the charge radius change is related to the difference of intrinsic quadrupole moments Q_0 of the considered isotopes. Thus, there can be a substantial radius increase if the charge distribution of one isotope is more deformed than the other even if their volumes are nearly the same.

Already in 1934 Schüler and Schmidt [18] found an anomalously large isotope shift between the spectral lines of the spin $I = 0$ nuclei ^{150}Sm and ^{152}Sm , which was nearly twice as large as between neighboring isotope pairs, of mass number 148 – 150 and 152 – 154. This large shift could not be explained by a pure volume effect ⁶. The explanation offered by Brix and Kopfermann in 1947 [19] is based on the following idea: (i) the anomalous isotope shift is connected with the jump of the quadrupole moments between ^{151}Eu and ^{153}Eu , and (ii) the $I = 0$ nuclei ^{150}Sm and ^{152}Sm have approximately the same intrinsic deformation as the ^{151}Eu and ^{153}Eu nuclei with $I = 5/2$. In other words, they assumed that the spectroscopic quadrupole moments observed in the europium isotopes were already present in the samarium isotopes. This seemed reasonable because the large quadrupole moments of the europium isotopes could not possibly be generated by the addition of a single proton to the corresponding samarium nuclei. With this assumption they could explain the observed large isotope shift between the two samarium isotopes.

⁶A pure volume effect would give a radius change of $\delta \langle r^2 \rangle = 0.21 \text{ fm}^2$, whereas the observed value was approximately $\delta \langle r^2 \rangle = 0.48 \text{ fm}^2$.

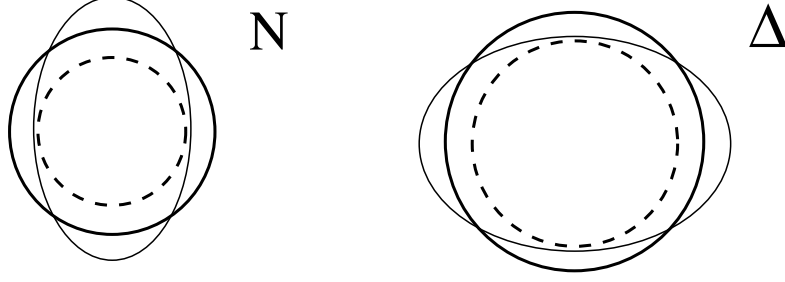


Figure 6: Decomposition of the N and Δ charge radii into a volume and a deformation contribution. The intrinsic quadrupole deformation of the nucleon and Δ leads to an increase of the proton (left) and Δ^+ (right) charge radii. The broken lines correspond to the spherical volume contribution. The deformation contribution to the charge radii indicated by the thin ellipsoids is given by the negative of the neutron charge radius according to Eq.(19). The full circles represent the measured charge radii which contain the effect of averaging the deformed charge distribution over all directions in space.

4.3 Estimate of the nucleon deformation contribution to hydrogen hyperfine structure

Applying these ideas to the nucleon, we decompose the proton and Δ^+ charge radii in two terms, a spherically symmetric volume contribution and a deformation contribution due to the intrinsic quadrupole charge density (see Fig. 6). This corresponds to the decomposition in Eq.(11). The deformation contribution to the proton and Δ^+ charge radii, which makes the charge radius bigger, is determined by the neutron charge radius

$$\begin{aligned} r_p^2 &= r_{p,vol}^2 + r_{p,def}^2, & r_{\Delta^+}^2 &= r_{\Delta^+,vol}^2 + r_{\Delta^+,def}^2 \\ r_p^2 &= r_p^2 + r_n^2 + (-r_n^2), & r_{\Delta^+}^2 &= r_p^2 + (-r_n^2). \end{aligned} \quad (19)$$

If written in this way we see that the volume contribution to the proton charge radius is given by the isoscalar charge radius $r_{p,vol}^2 = r_{IS}^2$. The latter is defined in terms of the proton and neutron charge radii as $r_{IS}^2 =: r_p^2 + r_n^2$. The deformation contribution to the proton charge radius is given by the negative of the neutron charge radius $r_{p,def}^2 = -r_n^2$. Similarly, the volume contribution to the Δ^+ charge radius is given by $r_{\Delta^+,vol}^2 = r_p^2$, and the deformation contribution is (as in the case of the proton) given by $r_{\Delta^+,def}^2 = -r_n^2$.

In the quark model the isoscalar charge radius is mainly determined by the quark core radius $b \approx 0.6$ fm and the charge radius of the constituent quark $r_q \approx 0.6$ fm

$$r_{IS}^2 = b^2 + r_q^2. \quad (20)$$

The quark core of the nucleon and the constituent quarks themselves are assumed to be spherical. Concerning the quark core, this is supported by explicit calculation of the P and D wave probabilities in the nucleon wave function, which are very small [8]. The deformation of the nucleon arises predominantly from the collective quark-antiquark degrees of freedom described by the two-body operators of section 2.2.

To estimate the energy shift of s electrons in atomic hydrogen which results from the deformation of the nucleon's charge density we use $\delta \langle r^2 \rangle = -r_n^2$ in Eq.(18). For $n = 1$ and $a_0 = 0.529 \text{ \AA}$ we then obtain

$$\delta E_{IS}(\text{def}) = 157 \text{ kHz.} \quad (21)$$

Compared to other corrections in the hydrogen hyperfine structure [20] this seems to be a big effect. We emphasize that this deformation contribution is already included in the experimental proton charge radius [21]. One possibility to isolate the deformation contribution to the proton charge radius is to measure hydrogen isotope shifts. The increasing accuracy of such experiments [22] will perhaps reveal some discrepancies between theory and experiment that arise from the intrinsic deformation of the hydrogen isotopes, and which manifest themselves as deformation contributions to their charge radii. In this connection we mention that the proton charge radius as determined in hydrogen Lamb shift measurements may be principally different from the one determined in elastic electron-proton scattering. Atomic physics experiments involve small electronic line widths and thus measure the electromagnetic interaction of the bound electron with the proton over long time scales. Thus they see a time average of the proton's deformed charge distribution. Because of this averaging effect they yield a bigger proton charge radius. On the other hand, high energy electrons involve comparatively short interaction times, which corresponds to taking a snapshot of the deformed charge distribution having a particular orientation in space and thus see a slightly smaller charge radius.

5 Summary

In summary, the electromagnetic excitation of the nucleon to its first excited state, the Δ resonance, has provided clear evidence that the charge distribution of the nucleon deviates from spherical symmetry. The intrinsic quadrupole moment of the nucleon, which is defined

with respect to a body-fixed coordinate system that co-rotates with the nucleon, is a measure of the nucleon's quadrupole deformation. We have calculated the intrinsic quadrupole moment of the nucleon in the quark model and found that it is given by the neutron charge radius, implying a prolate deformation of the nucleon's charge distribution. More generally, we have suggested that the neutron charge density $\rho^n(r)$ is a measure of the intrinsic quadrupole charge density of the nucleon $\rho_{def}^p(r)$.

Isotope shifts of atomic spectral lines have provided information on the intrinsic deformation of spin 1/2 and spin 0 nuclei, which do not have spectroscopic quadrupole moments due to angular momentum selection rules. The hydrogen spectrum can be measured with very high accuracy. It does not seem completely unlikely that some future experimental technique, perhaps involving muonic hydrogen, or hydrogen molecules, such as H_2 , HD , and D_2 , will reveal further nucleon structure details such as the spatial shape of the proton.

References

- [1] S. G. Karshenboim. Can. J. Phys. 77, 241 (1999).
- [2] A. M. Bernstein. Eur. Phys. J. A **17**, 349 (2003); arXiv:hep-ex/0212032.
- [3] L. Tiator, D. Drechsel, S.S. Kamalov and S.N. Yang. Eur. Phys. J. A **17**, 357 (2003).
- [4] G. Blanpied, M. Blecher, A. Caracappa *et al.*. Phys. Rev. C **64**, 025203 (2001).
- [5] A.J. Buchmann and E.M. Henley. Phys. Rev. C **63** (2001) 015202; Phys. Rev. D **65**, 073017 (2002).
- [6] H. Frauenfelder and E.M. Henley. Subatomic Physics. Prentice Hall, Englewood Cliffs, 1974.
- [7] A. J. Buchmann and E. Hernández, A. Faessler. Phys. Rev. C **55**, 448 (1997).
- [8] A. Buchmann, E. Hernández, and K. Yazaki. Phys. Lett. **B 269**, 35 (1991); Nucl. Phys. **A 569**, 661 (1994).
- [9] A.J. Buchmann, J.A. Hester, R.F. Lebed. Phys. Rev. D **66**, 056002 (2002).

- [10] S. Kopecky, P. Riehs, J. A. Harvey, and N. W. Hill *et al.*. Phys. Rev. Lett. **74**, 2427 (1995).
- [11] A.J. Buchmann, Phys. Rev. Lett. **93**, 212301 (2004).
- [12] A. Bohr and B. Mottelson. Nuclear Structure II, W. A. Benjamin, Reading (1975).
- [13] S. Galster, H. Klein, J. Moritz, K. H. Schmidt, D. Wegener, and J. Bleckwenn. Nucl. Phys. **B 32**, 221 (1971).
- [14] P. Grabmayr and A.J. Buchmann. Phys. Rev. Lett. **86**, 2237 (2001).
- [15] J.M.B. Kellogg, I.I. Rabi, N. F. Ramsey Jr., J.R. Zacharias. Phys. Rev. **55**, 318 (1939).
- [16] P. Brix. Z. Naturforsch., **41A**, 3 (1986). This paper reviews the history of the discovery of nuclear and intrinsic quadrupole moments.
- [17] H.B.G. Casimir. On the interaction between atomic nuclei and electrons. W.H. Freeman, San Francisco, 1963
- [18] H. Schüler and Th. Schmidt. Z. Phys. **92**, 148 (1934).
- [19] P. Brix and H. Kopfermann. Z. Phys. **126**, 344 (1949).
- [20] A. Dupays, A. Beswick, B. Lepetit, C. Rizzo, D. Bakalov. Phys. Rev. A **68** (2003) 052503; R. Rosenfelder. Phys. Lett. **B 463**, 317 (1999); J. L. Friar and I. Sick, Phys. Lett. **B 579**, 285 (2004).
- [21] Th. Udem, A. Huber, B. Gross, J. Reichert, M. Prevedelli, M. Weitz, and T. W. Hänsch. Phys. Rev. Lett. **79**, 2646 (1997).
- [22] A. Huber, Th. Udem, B. Gross, J. Reichert, M. Kouroggi, K. Pachucki, M. Weitz and T. W. Hänsch. Phys. Rev. Lett. **80**, 468 (1997).